J Mater Sci (2008) 43:5456–5469
DOI 10.1007/s10853-008-2829-1

Cooling slope casting to obtain thixotropic feedstock II: observations with A356 alloy

E. Cardoso Legoretta · H. V. Atkinson · H. Jones

Received: 18 December 2007 / Accepted: 24 June 2008 / Published online: 16 July 2008

Abstract New Rheocasting (NRC) is a recently developed semisolid processing route. There are two versions of this route. In one, molten alloy is poured directly into a mould and through careful temperature control during cooling a spheroidal semisolid microstructure is achieved, before the material in the mould is upended into a shot sleeve and hence forced into a die. Alternatively, the molten alloy is poured onto a *cooling slope* and thence into a mould before processing. The aim of the work described in this paper, and its companion, was to develop the understanding of the microstructural development during the initial stages of this process, i.e. in the mould before processing and with the cooling slope/mould combination. In the previous paper, an analogue system based on aqueous ammonium chloride has been used to visualise what happens when an alloy is poured into a tilted mould with a chill wall, which acts to mimic the mould and the cooling slope in the NRC process. In this companion paper, the results for pouring A356 aluminium alloy directly into a mould, and also via a cooling slope into a mould, are presented.

E. C. Legoretta
Centro de Investigaciones en Materiales y Metalurgia, Cuidad Universitaria, Universidad Autónoma del Estado de Hidalgo, Carretera Pachuca-Tulancingo Km. 4.5, Pachuca, Hidalgo, Mexico

E. C. Legoretta · H. Jones
Department of Engineering Materials, University of Sheffield, Sir Robert Hadfield Building, Mappin Street, Sheffield S1 3JD, UK

H. V. Atkinson (✉)
Department of Engineering, University of Leicester, University Road, Leicester LE1 7RH, UK
e-mail: hva2@le.ac.uk

Introduction

In the companion paper [1], a detailed background is given. Here this will be briefly summarised.

Thixotropy was first discovered in semisolid metallic systems in the early 1970s [2]. If the microstructure in the semisolid state consists of spheroids of solid in a liquid matrix, rather than dendrites, the material will flow when sheared but thicken if it is allowed to stand. Such a microstructure is termed 'thixoformable'. Reviews are given in [3–7]. Manufacturing routes based on this behaviour are termed semisolid processing. One particular route, which is industrially exploited, is the New Rheocasting (NRC) process patented by UBE [8, 9]. This is summarised in Fig. 1 of Ref. [1]. In one version of the route molten alloy is poured via a *cooling slope* (see Fig. 1 step [1]-a of Ref. [1]) into a tilted steel mould (which moves to the vertical during the process) and in the other the pouring is direct (see Fig. 1 step [1]-b of Ref. [1]). In subsequent steps, the semisolid is cooled slowly (see Fig. 1 in this paper), allowing the development of a fine, uniform spheroidal microstructure. It is then delivered, whilst still in the semisolid state, into the shot sleeve. Advantages include the fact that there is no need for specially treated thixoformable feedstock and scrap can be readily recycled within the plant [10]. The main disadvantage is that the mould size and mould induction heating conditions are necessarily very precisely related to the metered volume of alloy. Thus, the process is highly suitable for volume production but less suitable for producing components of varying sizes where, each time the size changed, a different mould would be required.

Previous researchers have shown [11] that it is important to hold the melt close to the liquidus temperature and to quench it quickly to form many nuclei. These are

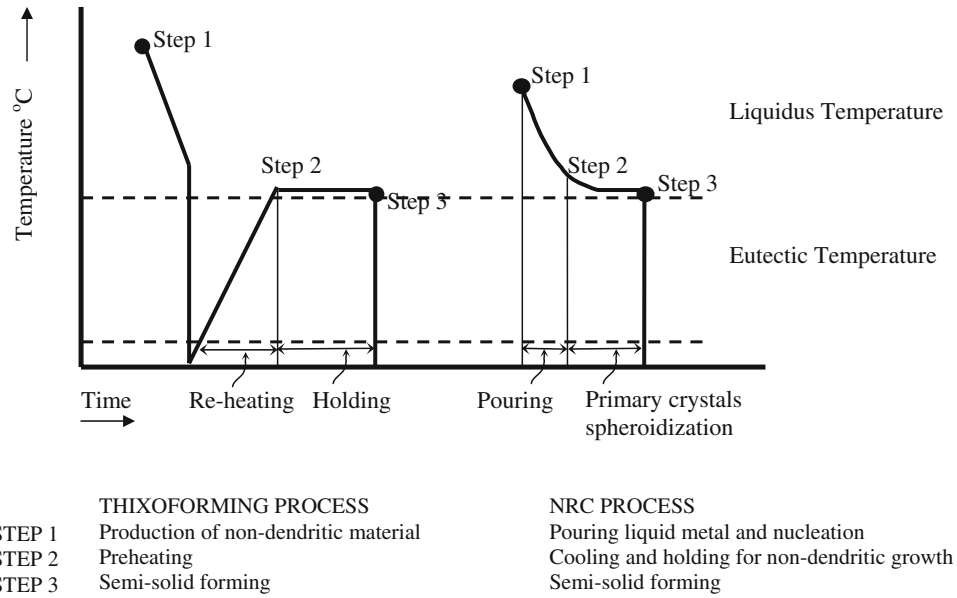

	THIXOFORMING PROCESS	NRC PROCESS
STEP 1	Production of non-dendritic material	Pouring liquid metal and nucleation
STEP 2	Preheating	Cooling and holding for non-dendritic growth
STEP 3	Semi-solid forming	Semi-solid forming

Fig. 1 Temperature versus time for thixoforming and NRC processes

distributed throughout the cup (the mould in Fig. 1 of Ref. [1]) and grow in a globular fashion when two criteria are both fulfilled—the nuclei must be small and the temperature gradient in the cup shallow. Dendritic growth then does not develop and the behaviour is very similar to that in liquidus casting [12]. Uggowitzer and Kaufmann [13] argued that the nuclei are formed by partial quenching of the melt. This was backed up by simulation results from Zhu et al. [14]. One central aspect of the NRC process [11] is the laminar filling of the crucible, which is achieved by controlled pouring of the melt along the wall of the inclined crucible (see Fig. 1 [1]-b of Ref. [1]). The microstructure is distinctly more dendritic after turbulent filling, i.e. uncontrolled direct pouring into the centre of the cup.

For the cooling slope, Mitsuru et al. [15] have proposed that particle multiplication occurs as the dendrites that are growing on the surface are fractured by the shear stress produced by the fluid flowing down the slope. A change in tilt angle would change the fluid flow rate and alter the extent of this phenomenon. Lee et al. [16] found that increased flow velocity increased the deflection of dendrites growing on a tilted chill plate. This fluid flow resulted in plastic deformation or partial melting of the growing dendrites and their detachment from the cooling slope, with the crystals being carried into the mould.

The use of a cooling slope to generate non-dendritic semisolid microstructures is gaining increasing attention for a range of processing routes other than the NRC process. Haga et al. [17] showed that the solid fraction entering the mould from the slope increased with the length of contact of the melt with the cooling slope. Haga [18] has linked the cooling slope to feed twin roll casters and other researchers have fed the material to strip rollers [19]. A number of researchers have characterised material produced with a cooling slope [20–22], or have used such material to produce semisolid processed components for mechanical characterisation [23]. Recently, there has been interest in applying the cooling slope to high-temperature alloys such as steels, where protective gaseous atmospheres should be applied to minimise oxidation [24, 25]. In addition, vibration has been applied to a cooling slope, albeit one where a transparent analogue is being employed [26]. The principal objective of vibration is to increase the number of nuclei available by fragmentation or by stimulation of free nucleation in the liquid. Note that in this paper, the flow down the slope is videoed and the material left on the slope examined after pouring (the 'remnant material'). These observations have not been reported in any previous work. In addition, none of the previous researchers have described a bottom-stoppered arrangement for pouring onto the slope.

In the companion paper [1], work with a transparent analogue is described, illustrating graphically the processes as a near-liquidus melt enters a mould with the lower wall chilled. In the transparent analogue, the crystals are significantly denser than the liquid and tend to settle through the liquid and also roll down the chilled wall. Increasing tilt angle tends to increase the speed at which particles roll down the wall and therefore enhances the possibility of equiaxed formation rather than columnar dendritic growth. There will be an optimum angle for enhancing equiaxed formation beyond which the chill wall is not playing as significant a role in nucleation.

In this paper, A356 aluminium alloy has been used and the following characterised systematically: effect of mould

type, superheat, use of a heated mould, pouring temperature, cooling slope length, cooling slope tilt angle and slope temperature. The influence of vibration and of rotating the mould has also been examined. It was thought that rotation of the mould might enhance spheroidal development.

Experimental method

Cooling slope apparatus

Initially, top pouring from an alumina crucible was used but the flow onto the slope was very uncontrollable. A second arrangement involved pouring the treated melt via a small tundish, but here close temperature control was difficult. In the final setup, as shown in Fig. 2a, for optimum control of the flow and temperature during casting, a bottom-stoppered alumina crucible with a graphite nozzle was used. The details are shown in Fig. 2b, c. During melting, the nozzle was stoppered with a ceramic (mullite or alumina) rod, within which a K-type thermocouple was located to monitor the temperature during the melting and teeming process. Flow down the slope was videoed with a high-speed JVC digital camera. Thermocouples (K-type) were used to monitor the temperature at the beginning and the end of the cooling slope, making sure that the flowing metal was in contact with them. Three different casting distances ('cooling lengths') were evaluated (250, 200 and 150 mm) in conjunction with a stainless steel mould. The mould at the bottom of the slope (dimensions given in Table 1) had sides with a draft angle of 3° to help removal of the ingot following solidification. The mould was vertical and the base of the slope above it was such that semimolten metal flowed into the middle of the cup. Here, the role of the cooling slope is focussed on, rather than the tilt of the mould. In order to avoid sticking of the metal to the cooling slope (which was made of mild steel) and the mould, boron nitride was sprayed on their surfaces.

Melting was carried out with a Banyard medium frequency induction furnace (50 kW maximum power and frequency up to 9,600 Hz). A charge of $\sim$1 kg of aluminium alloy was melted at 700 °C and held for 5 min for temperature homogenisation. Then a hexachloroethane tablet was added to reduce the hydrogen content before pouring down the cooling slope. Casting temperatures were varied between 620 and 680 °C.

For most experiments, the cooling slope had cold water circulating through it. The effect of altering the temperature of the cooling slope was examined. The conditions were: (a) slope preheated to 400 °C, (b) slope at room temperature (20 °C) but with no cold water circulating through it and (c) slope chilled with cold water circulating. The effect of altering the temperature of the mould was also examined. For the 'cold' mould, the mould was at room temperature. The casting procedure was to pour the molten metal down the slope and let it run into the mould. The mould and contents were then quenched directly. In the hot mould experiments, the mould was previously heated to the desired temperature (in this case 400 °C) in an electric resistance furnace and then transferred to another vertical cylindrical resistance furnace pre-set at 580 °C to allow isothermal holding in the semisolid condition (see Fig. 3, which also shows the vibratory device which is described in section 'vibration of the slope and rotation of the mould'). The furnace and the mould within it were located at the end of the cooling slope. The aluminium alloy was poured into the mould via the cooling slope and then the mould quenched after the required holding time.

For comparison with cooling slope results, some ingots were cast directly into the mould without the cooling slope. The temperature of the mould was room temperature and the pouring temperatures were 620, 630 and 650 °C. In contrast with the cooling slope experiments, the crucible was top poured into the mould (this was to avoid disassembling the cooling slope apparatus). For comparison purposes, the mould materials were varied (see Table 1). The wall thicknesses also varied and, in the case of the insulator mould, the dimensions were also different (50 mm internal diameter $\times$ 50 mm height, cf. 40 mm internal diameter $\times$ 70 mm height for the other mould materials). The mould was insulated with MgO bricks on the top and on the bottom to favour radial heat extraction. A K-type thermocouple was located centrally at the mid-height of the mould cavity and its output recorded with rapid data acquisition software. The stainless-steel mould was found to give the best results and was therefore used for all subsequent experiments.

Vibration of the slope and rotation of the mould

Two modifications were incorporated with the objective of aiding nucleation. Firstly a sieve shaker with 60 Hz frequency was attached to the slope to apply horizontal vibration whilst the metal was being cast down it. The second was to rotate the mould at 200 rpm. Figure 3 shows the experimental set up for the vibration device.

Materials and metallography

The A356 alloy was supplied by Alcan (6.82 Si, 0.32 Mg, 0.22 Cu, 0.005 Zn, 0.112 Fe, <0.005 Mn, 0.10 Ti, 0.013 Pb, 0.042 Sn, 0.006 Ni, 0.005 Cr, balance Al). The liquidus is at 615 °C and the solidus at 577 °C [27].

The small ingot samples from the cooling slope and direct casting experiments were sectioned vertically. The locations of images are then described as 'edge', 'mid-

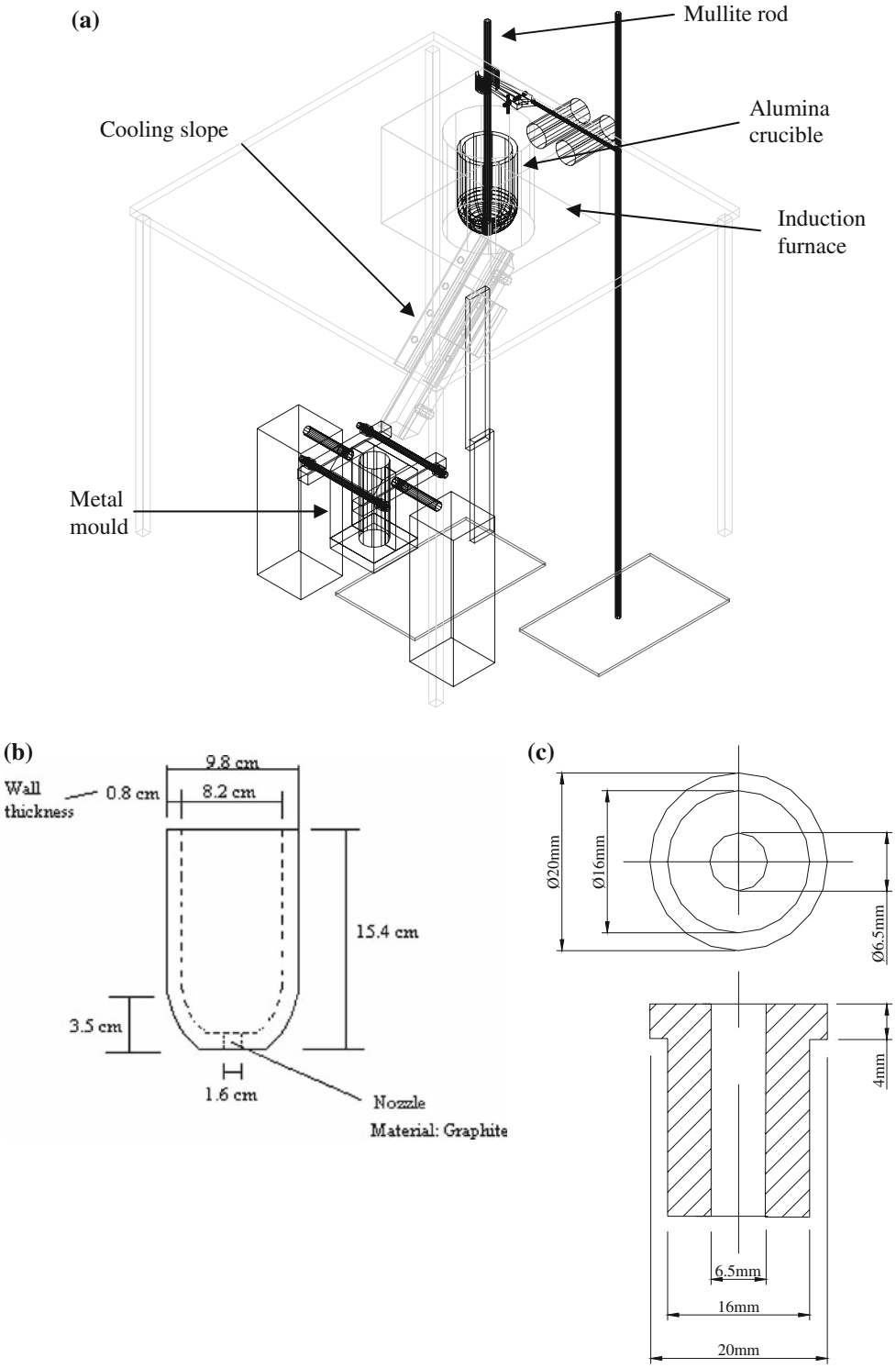

Fig. 2 (**a**) Cooling slope with bottom pouring from the alumina crucible and tilting mould. (**b**) Detail of alumina crucible. (**c**) Detail of nozzle at the base of the alumina crucible

radius' and 'centre'. For metallography, all specimens were mounted in bakelite, polished using 240 and 600 grinding papers, and then polished with 6 and 3 μm diamond pastes followed by ¼ μm 'Silco' liquid. Electrolytic anodising was carried out with the sample as the anode and a stainless-steel wire as the cathode. Barker's reagent (5 mL HBF_4 (48%), 95 mL H_20) was used as the electrolyte. The voltage was set at 20 V and the samples were held for 1.5–2 min.

In addition to the ingot microstructures, top, middle and end-of-slope microstructures were obtained from remnant metal solidified on the cooling slope.

Table 1 Different mould materials used in the A356 experiments

Material	Wall thickness (cm)	Internal diameter (cm)	Mould height (cm)
Copper	1.4	4	7
Stainless steel type 304	0.5	4	7
Mild-steel	1.5	4	7
Insulator mould (calcium silicate $CaO–SiO_2$)	2.4	5	5

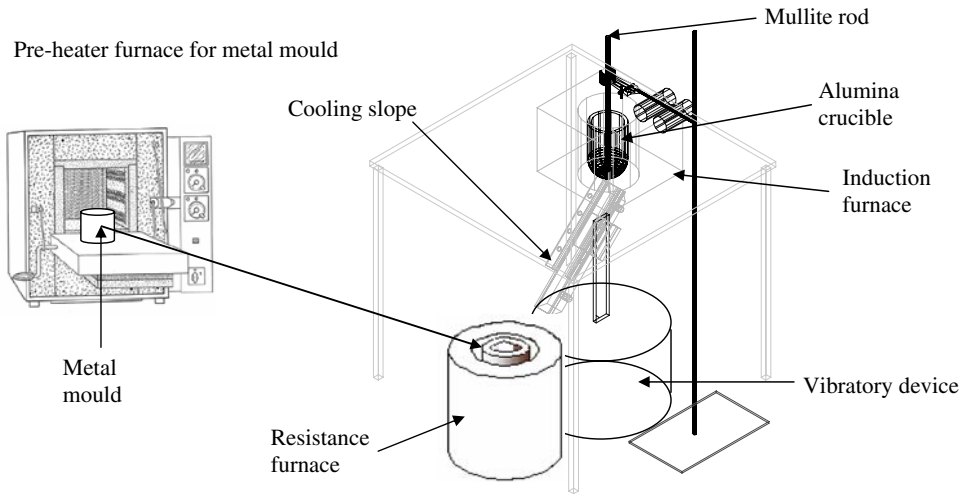

Fig. 3 Bottom pouring onto a vibrating cooling slope (and with casting into a preheated mould)

Image analysis was carried out on microstructures using Sigma Scan Pro 5 (a commercial software package) to determine the area and perimeter of α-Al particles. Note that this is cell size rather than grain size, i.e. each globule is treated as a separate entity. The shape factor was defined as $(\text{perimeter})^2/4\pi(\text{area})$. For optimum semisolid processing characteristics, the shape factor should be as close to 1 as possible. The error on shape factor measurements is about ±0.1. Particle sizes were measured by the linear intercept method according to the ASTM E112-96 standard. The error on particle size measurements is about ±3 μm unless stated to be otherwise. Volume fraction solid was predicted using the Scheil equation assuming binary composition Al–Si alloy.

Experimental results

The basic effect of the cooling slope

Figure 4 shows the characteristic dendritic growth which results from conventional casting into a metal mould with no cooling slope. The superheat was high enough to ensure that the number of crystals nucleated was insufficient to produce fine spheroidal primary crystals; instead coarse non-spheroidal crystals were formed. When the molten alloy was cast via the cooling slope into a metal mould at room temperature, small compact primary α-Al crystals were formed, the resulting microstructure showing dendritic character towards the edge, rosettes at mid-radius and rosettes and spheroids in the centre (Fig. 5).

Mould type

Figure 6 shows that mild-steel and copper gave the highest cooling rate, whilst stainless steel gave an intermediate rate and the insulating mould the lowest rate. It should be noted though that, above the solidus temperature of 577 °C, the cooling rates for all except the insulating mould are very similar. Figure 7 shows the microstructure obtained in four different cold moulds. A high thermal conductivity mould gives a small primary particle size in the centre (~65 μm for the copper mould). The primary crystals in the centre of the insulating mould are much larger (~135 μm).

Effect of superheat on ingot microstructure

Figure 8 shows the effect of superheat on particle size and shape factor. The particle size in the centre of the ingot was fairly constant, with change in pouring temperature, at between 70 and 75 μm. However, the shape factor in the centre of the ingot varies between 1.4 for a pouring temperature of 620 °C (i.e. strongly spheroidal) and 2.6 for 680 °C (i.e. predominantly dendritic). At the surface of the ingot,

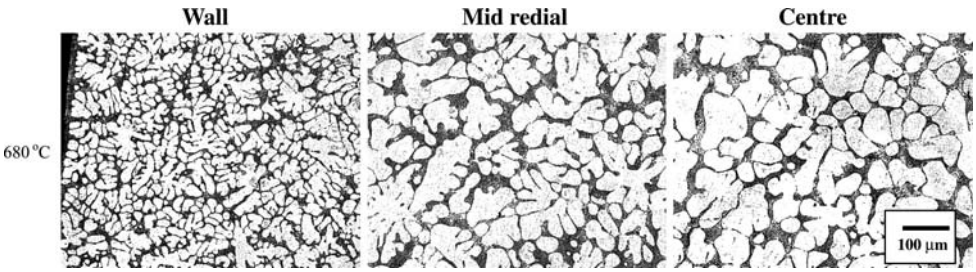

Fig. 4 Microstructure of A356 ingot obtained with no cooling slope into a vertical cold stainless steel mould (40 mm internal diameter, 70 mm height), molten metal superheated 65 K

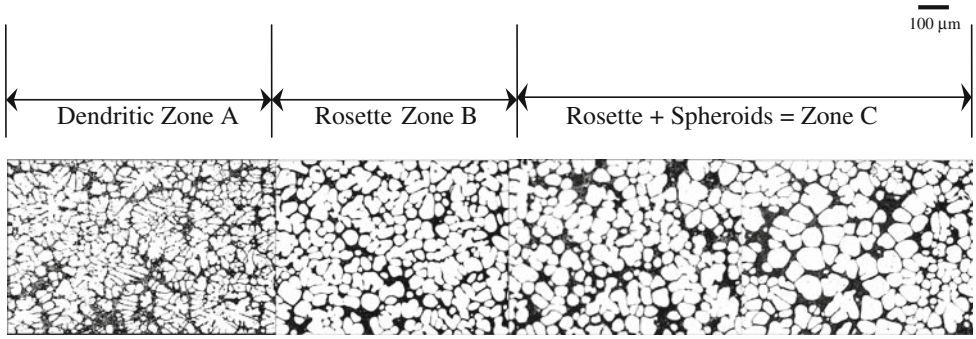

Fig. 5 Schematic illustrations of the microstructure zones in A356 alloy developed in a cold stainless steel mould, after pouring down the cooling slope. Superheat 10 K, cooling slope tilt angle of 60°

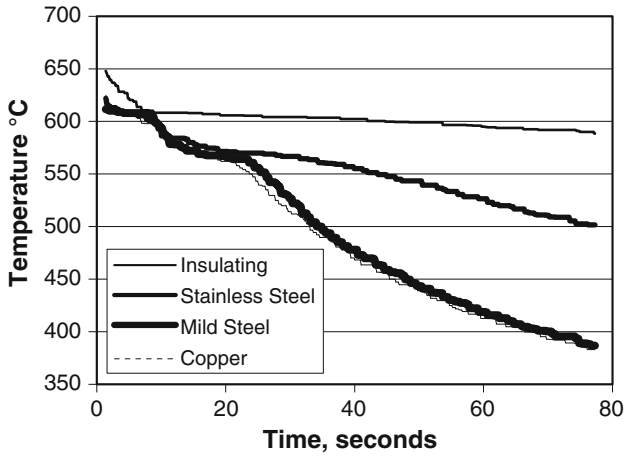

Fig. 6 Cooling curves for A356 with different mould materials. Molten metal superheated 35 K and poured directly into a vertical mould, mould dimensions as given in Table 1, thermocouple along the central axis of the mould

low superheat gave a much finer microstructure in comparison with higher pouring temperature (33 vs. 75 µm). The shape factor is always high (between 3.8 and 4.3) at the surface of the ingot and the structure is basically dendritic.

Microstructure with a heated mould

Results from pouring into a cold mould compared with those from pouring into a stainless steel mould at 300 °C and one at 400 °C show that, with increased mould temperature, the microstructure becomes coarser but not spheroidal. However, if the mould and contents are maintained in a furnace at a semisolid temperature, even for a short time, the microstructure becomes spheroidal and homogeneous. Figure 9 shows a microstructure which is representative of the structure right across the ingot. The average spheroid size is about 120 µm with a shape factor of 1.4. Figure 10a shows that teeming into a cold stainless-steel mould via 250 mm of cooling slope develops a rosette-like morphology with a particle size of ~70 µm and a shape factor of ~1.7. Figure 10b shows that teeming, via 250 mm of cooling slope, into a stainless-steel mould preheated to 400 °C and then held at 580 °C for only 60 s (as opposed to 10 min in Fig. 9) gives α-Al particles 90 µm in size with a shape factor of ~1.5. This morphology is appropriate for the SSM process. It is important to control the hold time at 580 °C to avoid excessive coarsening of the α particles.

Effect of cooling slope length

The effect of cooling slope length is shown in Fig. 11. The contact time of the melt with the cooling slope increases as the contact length increases. However, there is little systematic difference in the morphology and size of the particles once the material has arrived in the mould and been quenched. The particles in the centre have strong spheroidal morphology with a particle size of between 62 and 75 µm and a shape factor of between 1.2 and 1.4. Some indication of the reason for the lack of an effect of cooling slope length is shown in Fig. 12. Although these images are for a slope at 45° tilt angle rather than 60° (as in Fig. 11), the behaviour shown is characteristic. When the molten metal first touches the

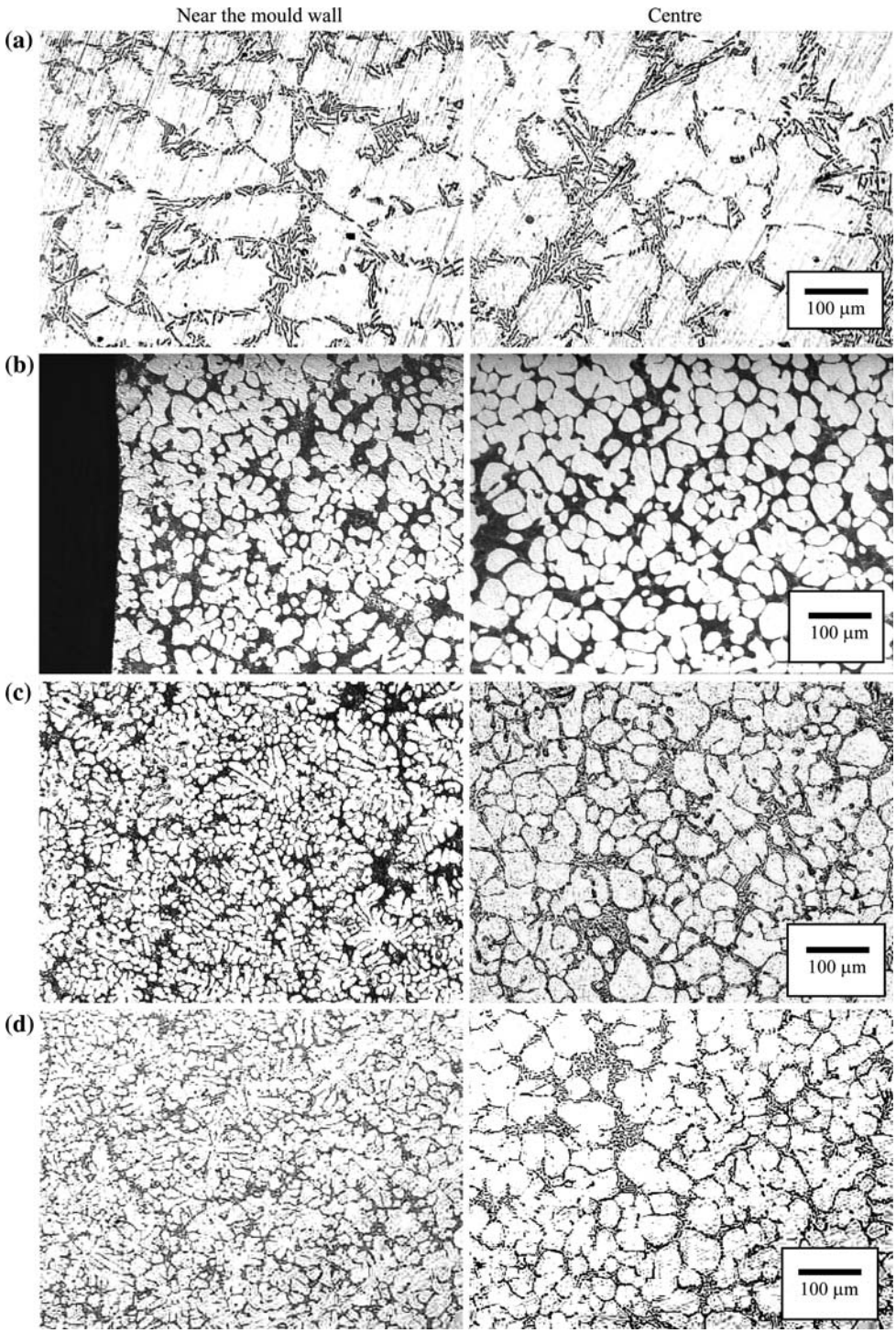

Fig. 7 Micrographs of the resulting microstructure of an A356 ingot obtained by pouring at 630 °C onto a cooling slope (length 250 mm) tilted at 60° and then flowing into moulds at room temperature made of four different mould materials. The micrographs are presented in order of increasing mould conductivity. (**a**) Insulating mould. (**b**) Stainless steel. (**c**) Mild-steel. (**d**) Copper

slope it forms an elliptical 'impact zone', where the material is spread. A short distance further down the slope, the alloy has regathered into a 'snake' and then progresses as a snake down the rest of the slope. The impact zone reaches its maximum area of extent (about 25 cm^2) in the first second after teeming and then decreases rapidly after the first second to about 12 cm^2.

Microstructure of the remnant material on the cooling slope, including the effect of tilt angle

The remnant material has not been quenched as such but it is in contact with the cooling slope with water circulating through it and the whole pouring process only takes a few seconds. Figure 13 shows the microstructure of the

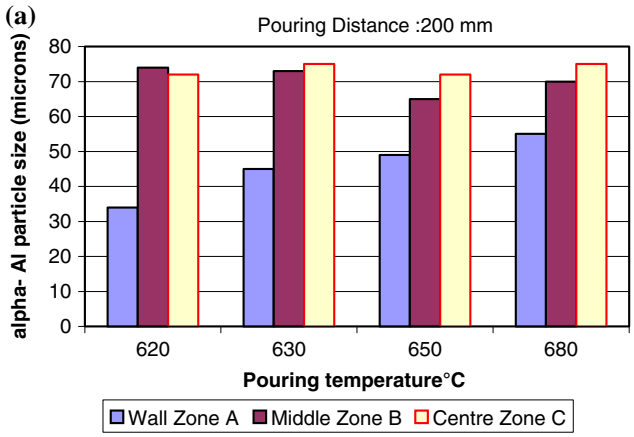

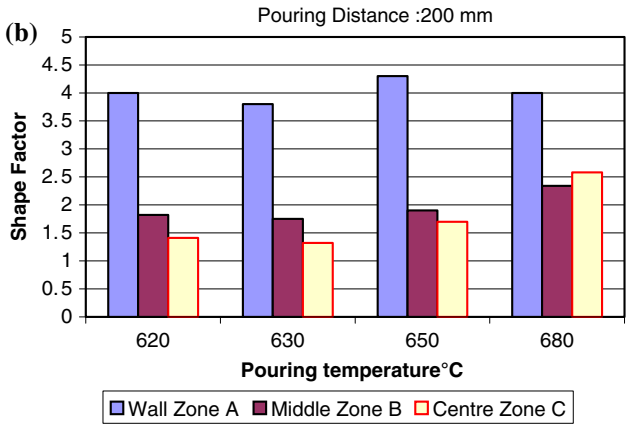

Fig. 8 Effect of pouring temperature on (**a**) α-Al particle size and (**b**) shape factor for A356, cooling slope tilt angle 60°, cold stainless-steel mould, slope distance 200 mm

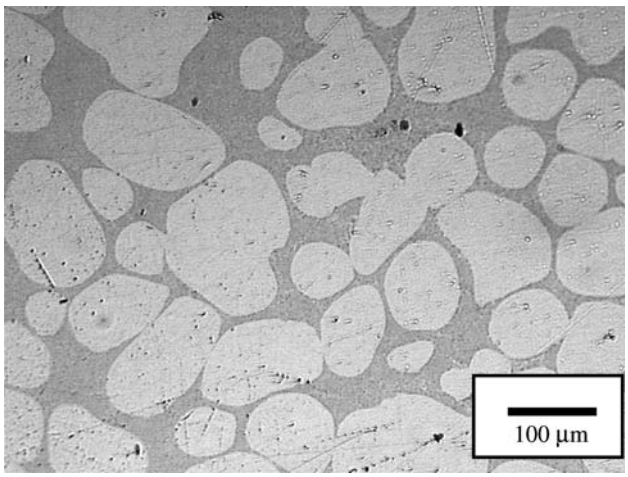

Fig. 9 Ingot microstructure of A356 poured at 620 °C down 250 mm of the cooling slope tilted at 60° and cast into the stainless-steel mould preheated to 400 °C then held for 10 min at 580 °C. (Location is in the centre of the ingot but this is representative of the structure throughout the ingot.)

remnant material for a cooling slope length of 250 mm. Figure 14 shows the effect of tilt angle and superheat on particle size and shape factor for a 250 mm slope length. The measurements were taken on microstructures from the bottom of the slope. The results for 60 and 45° are almost identical, with a slightly lower shape factor for 630 °C pouring than 620 °C. With a tilt angle of 30°, the shape factor is distinctly higher, with both pouring temperatures, than for the higher tilt angles. The grain size is slightly higher (80 µm as opposed to nearer 65 µm) for the low tilt angle than the higher ones at a 630 °C pouring temperature. At the 620 °C pouring temperature, the grain size is almost identical for all tilt angles.

Fraction solid at the end of the slope

Table 2 shows the loss of temperature during 250 mm travel down the slope. The time to travel down the slope was obtained from videos. The resulting cooling rate is given, along with the fraction solid at the end of the slope based on prediction from the Scheil equation. The fraction solid at the end of the slope was in the range 0.48–0.54 for a pouring temperature of 620 °C and 0.32–0.33 for 630 °C.

Effect of slope temperature

With the slope preheated to 400 °C, a relatively coarse structure was obtained in the ingot with a particle size at the centre of the ingot of 108 ± 32 µm and a shape factor of 1.3. If the slope was at room temperature (25 °C) the particle size and shape factor are almost identical to those with the chilled cooling slope (15 °C) viz ~85 ± 25 µm and 1.2. The pouring temperature for these experiments was 630 °C with a cooling slope length of 250 mm.

Vibration of the cooling slope and rotation of the mould

Comparing ingots produced with the vibration device and those without (pouring at 650 °C with a cooling slope tilt angle of 45° and a slope length of 250 mm), with a hold temperature in the ingot of 580 °C, shows the morphology to be very similar. There is, however, a measurable effect on the particle size (Fig. 15).

The microstructure obtained by teeming into a rotating mould is shown in Fig. 16 in comparison with that for a static mould. No cooling slope has been used. The ingot microstructure obtained with a static mould had a strong dendritic character (Fig. 16a, c). Close to the wall, a columnar dendritic morphology with dendrite arm spacing (DAS) of ~16 µm was observed. With the rotating mould, the microstructure at the wall is coarser (with a DAS of ~34 µm) (Fig. 16b, d). Table 3 shows that if a cooling

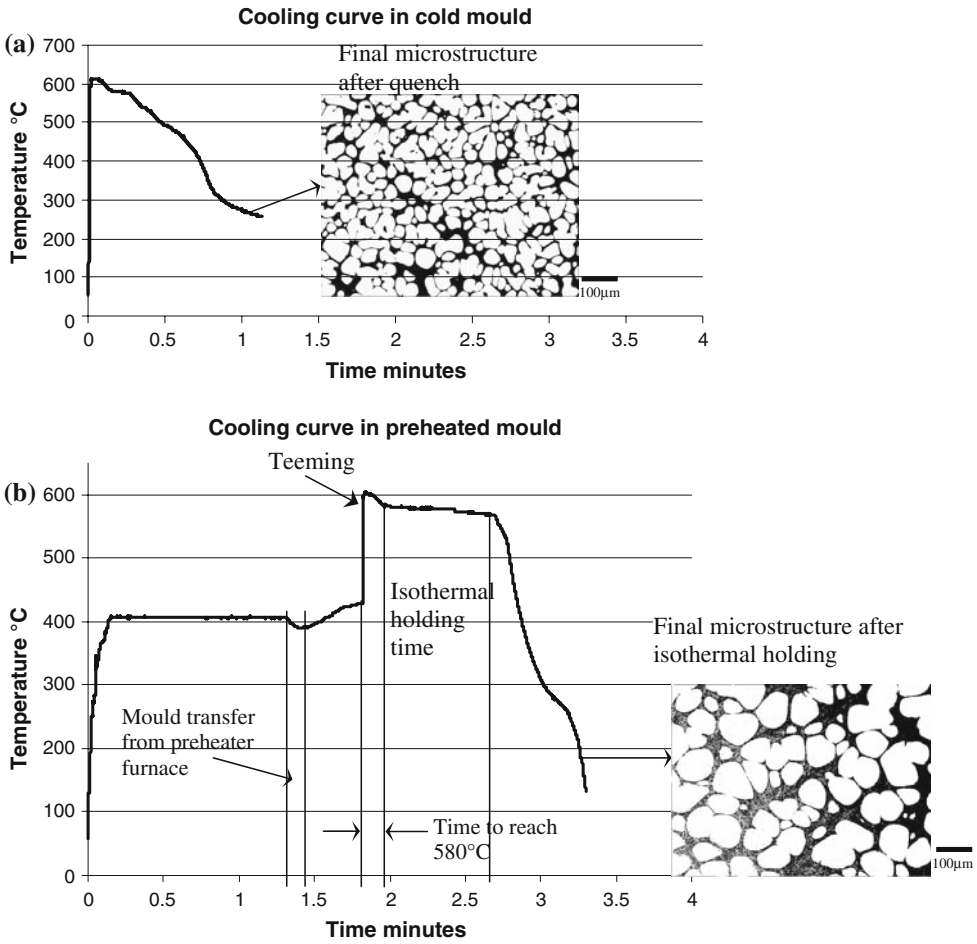

Fig. 10 A356 cooling curves in a stainless-steel mould at (**a**) 25 °C and (**b**) 400 °C. Molten metal poured at 620 °C, via cooling slope tilted at 60°. Thermocouple was suspended centrally in the mould

slope is used with the rotating mould the microstructure is finer and the shape factor is smaller.

Discussion

The results for the effects of the thermal properties of the mould, the melt superheat, the effect of heating the mould and the casting without a cooling slope are consistent with those of previous researchers [13, 28, 29].

The existence of an 'impact zone' has not previously been identified in the literature. The impact zone on the slope is thought to be the principal source of nuclei in the cooling slope experiments. There is evidence to support this from the ingots (Fig. 11) and from the remnant material (Fig. 13). In Fig. 11, the length on the cooling slope has a relatively small effect on the particle size and shape factor in the centre of the ingot. The microstructures in Fig. 13 support the hypothesis that the majority of the nucleation is taking place in the top part of the slope. If nucleation were occurring significantly as the material progresses down the slope after the impact zone the microstructure in Fig. 13b would be much finer than it is and a wider range of globule sizes would be expected (as some nuclei would have had longer to coarsen than others). Comparing Fig. 13a with Fig. 13b, some coarsening is occurring. The relatively small effect of tilt angle with low superheat (620 °C) shown in Figs. 14 and 15 is consistent with this hypothesis. As the superheat is increased, tilt angle does start to have an effect, initially on shape factor, a low tilt angle (30°) giving a higher shape factor. Only the results for relatively low superheats are presented here and other researchers have investigated higher values, concluding that either 45° [20, referring back to an older reference although this does not appear to deal with the angles indicated or the same material] or 60° [17] is optimum. With higher tilt angle, the fluid flow rate will tend to be high, with the nuclei tumbling in the fluid flow, precluding the formation of extensive dendrites and enhancing rosette/spheroidal morphology.

It was expected that an increase in nucleation would be obtained, and as a consequence smaller particle sizes, with longer cooling slope distances. This is not what was found in this study but these results are in contradiction with results from other authors. Haga et al. [17, 28, 30] show results where the length of contact with the cooling slope

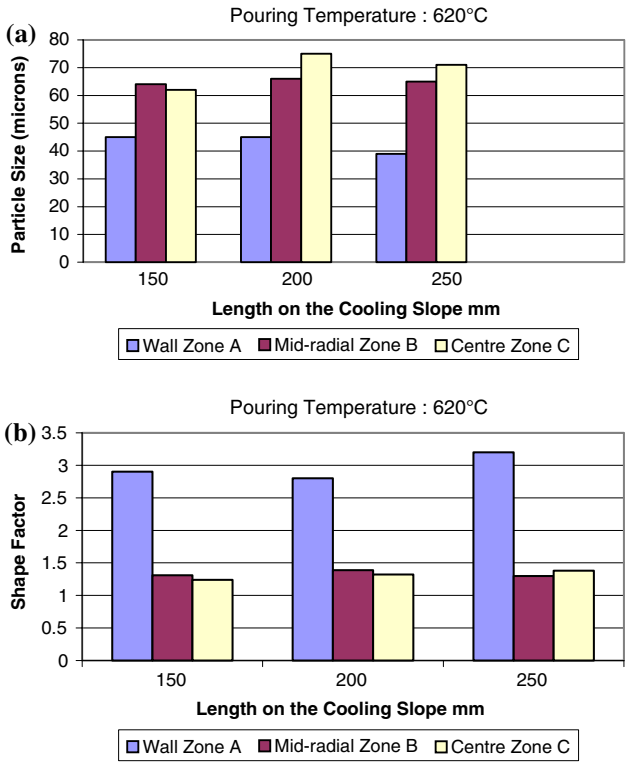

Fig. 11 Effect of the cooling slope length on (**a**) α-Al particle size and (**b**) shape factor for A356, cooling slope tilt angle 60°, pouring temperature 620 °C, cold stainless-steel mould

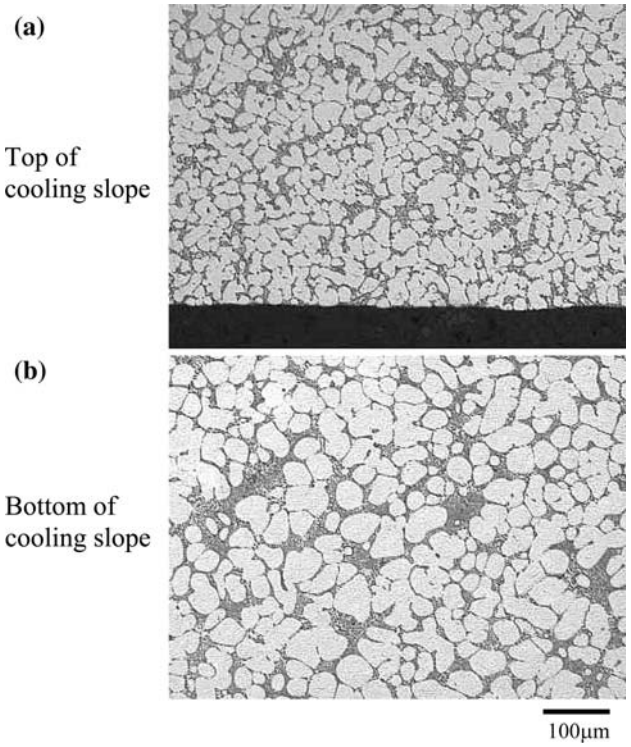

Fig. 13 Microstructure of the remnant A356 on the cooling slope tilted at 45° and poured at 630 °C with a cooling slope length of 250 mm

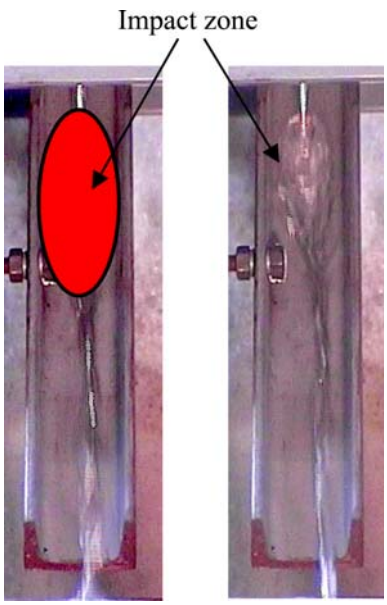

Fig. 12 Video images of the molten A356 running down the cooling slope. The length on the cooling slope is 250 mm and the pouring temperature 630 °C. The image is 0.32 s after the start of pouring. In this case the tilt angle is 45°

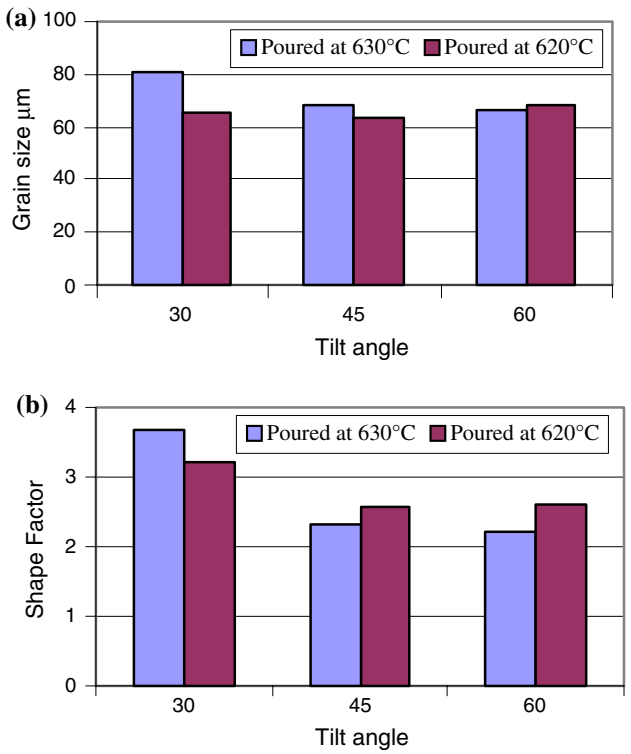

Fig. 14 Effect of cooling slope tilt angle on (**a**) α-Al particle size and (**b**) shape factor in remnant A356, 250 mm down the cooling slope

Table 2 Loss of temperature of A356 down the slope with slope length of 250 mm and tilt angle of 60° for different pouring temperatures

Pouring temperature (°C)	Temperature at the end of the slope (°C)	Temperature drop (K)	Time (s) to travel down slope	Cooling rate on slope (K/min)	f_s from Scheil equation
640	594	46	6.8	408	0.35
630	596	34	6.1	333	0.32
630	595	35	6.5	325	0.33
620	569	51	6.2	498	0.54
620	579	41	6.9	359	0.48

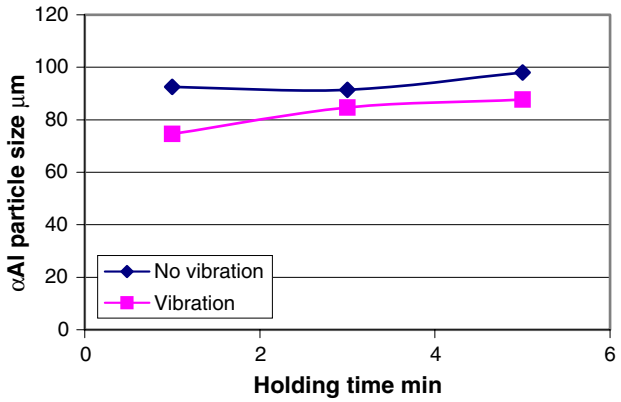

Fig. 15 Effect on A356 ingots produced with slope vibration and without slope vibration. Pouring temperature 650 °C, cooling slope tilt angle 45°, length of cooling slope 250 mm. Holding temperature 580 °C

does affect the ingot microstructure, although the effect was not quantified. Haga and co-authors used a cooling slope and cooling lengths very similar to that in this study, including the use of the boron nitride coating for lubrication. It should be noted, though, that the thickness of the boron nitride was not measured or standardised in this study and there is evidence in the literature that the thickness has an influence [29]. The role of the impact zone merits further investigation and experiments are currently underway on this.

Conventionally, the slope has been seen as a copious source of nuclei but it clearly plays a role in the spheroidisation process as well. Figure 13 shows that, on reaching the bottom of the cooling slope, some spheroidisation has occurred. The evidence from the remnant material suggests that there is little particle multiplication during travel down the slope (Fig. 13).

Huang et al. [26], in their work with a transparent analogue, have argued that vibration breaks down the solidification shell formed on the surface of the slope through rapid chilling and hence can produce finer globular grains in the resulting structure. The frequency and amplitude of vibration of the slope influence the outcome. Southin [31] suggests that, in comparison with a static surface, vibration enhances the showering of dendrites from the slope surface. Flemings [32] argues that success in achieving grain refinement through vibration is due to grain multiplication (by dendrite fracture or remelting) and not due to enhanced homogeneous nucleation. Here vibration has had a measurable effect on size (Fig. 15) but not shape. This suggests more nuclei are being produced but are then being subjected to similar shape governing processes.

The rotation of the mould is probably leading to detachment of the chilling solid as it forms at the wall. The rotation inhibits heat transfer (hence giving a coarser structure) but discourages the formation of the columnar dendritic zone (Fig. 16). The combination of a cooling slope with a rotating mould gives a structure which would be very suitable for semisolid processing with a size of 70 μm and shape factor of 1.4 (Table 3). However, without the rotation a size of 75 μm and a shape factor of 1.5 can be achieved. Rotation may not, therefore, be economically viable. It does however give greater homogeneity through the structure than without (Fig. 16). Comparing Fig. 16a and Fig. 16c, pouring direct into a static cold stainless-steel mould without a cooling slope, a pour temperature of 650 °C gives, if anything, a slightly finer microstructure than the 630 °C pour.

In the companion paper [1] for the transparent analogue, low superheat is shown to enhance the formation of fine, relatively spheroidal particles. The results in this paper are consistent with that. In [1], it is shown that the tilted chill wall is effective in promoting the formation of fine crystals (in comparison with a vertical arrangement). Again here, if the cooling slope is removed the microstructure tends to be coarser and more dendritic. In [1], increasing the tilt angle from 45 to 60° tended to enhance the possibility of equiaxed formation rather than columnar dendritic growth. Here the findings are more equivocal, with tilt angle showing relatively little effect, at least for low superheats. This is thought to be associated with the fact that, for the metallic system, the 'impact zone' is dominating the behaviour. The fact that the transparent analogue system consists of a cell rather than a slope means that this effect could not be observed in [1].

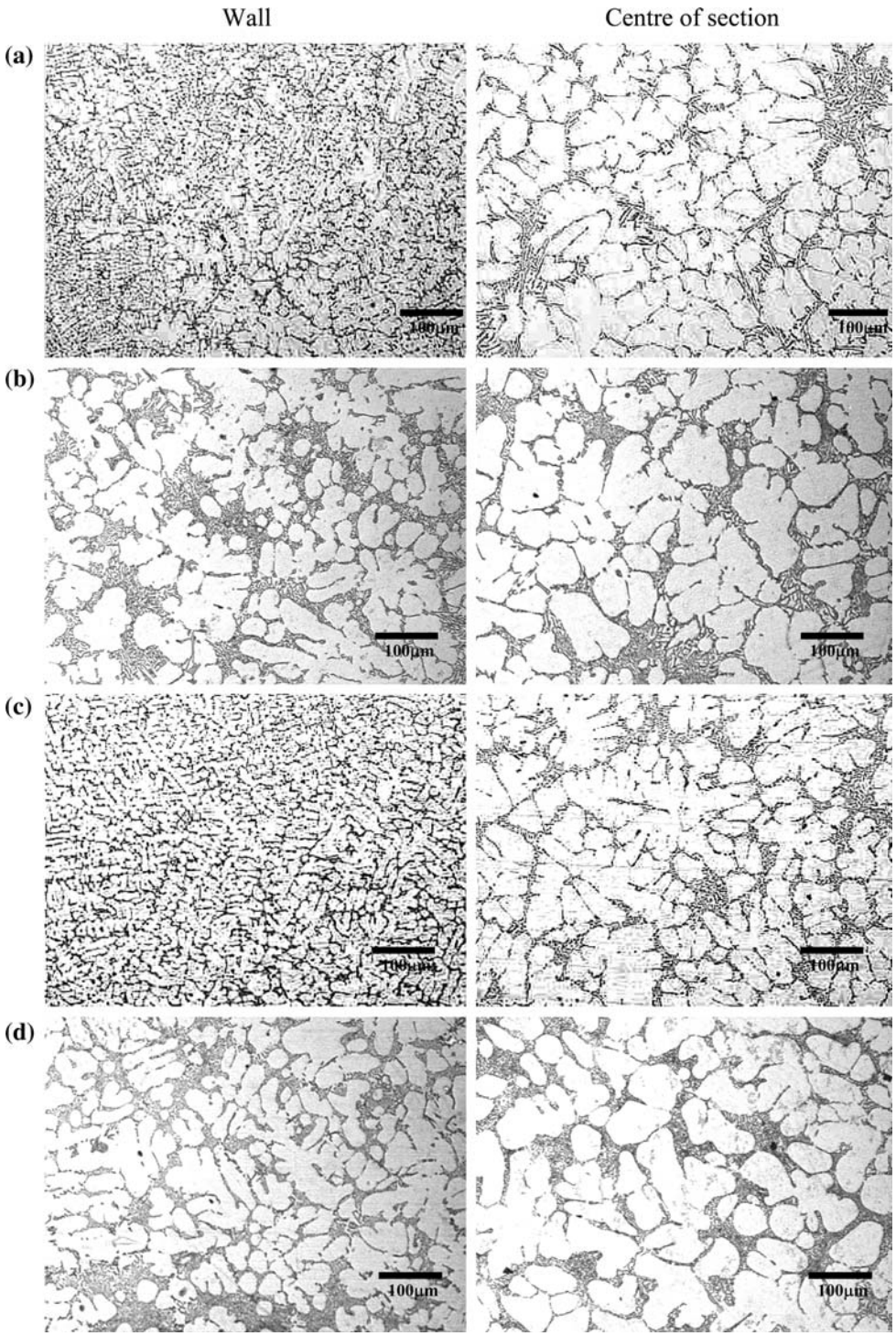

Fig. 16 Effect of rotating mould (with no cooling slope) on the A356 ingot microstructure (**a**) cold static stainless steel mould, pouring temperature 630 °C; (**b**) mould rotated at 200 rpm, pouring temperature 630 °C; (**c**) cold stainless-steel mould, pouring temperature 650 °C; (**d**) mould rotated at 200 rpm, pouring temperature 650 °C

Concluding remarks

The key findings from the above results are as follows.

(1) A high thermal conductivity mould gives a fine primary particle size in the centre of the ingot (65 μm with a copper mould) but an inhomogeneous microstructure across the ingot.

(2) Low superheat, with a cooling slope, gives fine, relatively spheroidal particles (70 μm and shape factor 1.4 for 5 °C superheat, 60° tilt, 200 mm cooling slope length) but again an inhomogeneous ingot structure.

(3) A heated mould gives a relatively coarse but non-spheroidal microstructure but a short hold at 580 °C in the semisolid region spheroidises the structure

Table 3 Effect of rotating the mould on the central part of the ingot microstructure with A356

Condition of mould	Teeming temperature (°C)	α-Al particle size (μm)	Shape factor
1	630	121 ± 16	2.4
2	630	102 ± 14	2.7
1	650	125 ± 28	1.8
2	650	109 ± 24	2.8
3	630	70 ± 18	1.4
4	630	75 ± 21	1.5

Where the cooling slope is used it is at 45° tilt angle and the distance on the slope is 250 mm

1, rotating stainless steel mould at 200 rpm. No cooling slope; 2, static stainless-steel mould. No cooling slope; 3, rotating stainless steel mould at 200 rpm and cooling slope; 4, static stainless-steel mould and cooling slope

(90 μm with a shape factor of 1.5 for a 400 °C mould); the microstructure is relatively homogenous across the ingot.

(4) Without a cooling slope, the microstructure tends to be coarser and more dendritic.
(5) The remnant material suggests there is little nucleation in the lower reaches of the slope but that some coarsening does occur as the material travels down.
(6) Tilt angle has relatively little effect, at least for low superheats.
(7) The slope could be used in the room temperature condition and get very similar results to those with the chill operating; a heated slope gives relatively coarse microstructures.
(8) Vibration is effective which is giving a finer particle size (by about 12 μm).
(9) A rotating mould gives a coarser structure but one which is less dendritic, particularly near the wall.

The results for the thermal conductivity of the mould, the melt superheat, the effect of heating the mould and the casting without a cooling slope are consistent with those of previous workers. There is some inconsistency in the results on tilt angle in comparison with those of other workers. This might be associated with issues in the quantification of microstructural features or the role of the impact zone at the top of the slope. It is hypothesised here that the elliptical impact zone may be the primary source of nuclei. These nuclei then coarsen and spheroidise during travel down the slope. Conventionally, the cooling slope has been seen as primarily causing heterogeneous nucleation but the results here suggest microstructural development occurs on the slope as well.

Acknowledgements E.C.L. would like to acknowledge financial support provided by CONACyt and SEP and also the Universidad Autónoma del Estado de Hidalgo for support. The authors are grateful to the Department of Engineering Materials at the University of Sheffield for the provision of laboratory facilities. In addition, we would like to thank Prof. T. Haga who built the initial version of cooling slope equipment at Sheffield University during a sabbatical period from the University of Osaka, and Dr. Plato Kapranos and Dr. Worawit Jirattiticharoean for experimental assistance. H.V.A. would like to thank the University of Leicester for sabbatical leave.

References

1. Legoretta EC, Atkinson HV, Jones H (submitted) J Mater Sci. doi:10.1007/s10853-008-2828-2
2. Spencer DB, Mehrabian R, Flemings MC (1972) Metall Trans 3:1925. doi:10.1007/BF02642580
3. Flemings MC (1991) Metall Trans A22:957
4. Kirkwood DH (1994) Int Mater Rev 39:173
5. de Figuredo A (ed) (2001) Science and technology of semi-solid processing. North American Die Casting Association, Rosemont, IL
6. Fan Z (2002) Int Mater Rev 47:49. doi:10.1179/095066001225001076
7. Atkinson HV (2005) Prog Mater Sci 50:341. doi:10.1016/j.pmatsci.2004.04.003
8. Kaneuchi T, Shibata R, Ozawa M (2002) In: Tsutsui Y, Kiuchi M, Ichikawa K (eds) Proceedings of the 7th international conference on advanced semi-solid processing of alloys and composites, Tsukuba, Japan, 2002. National Institute of Advanced Science and Technology and the Japan Society for Technology of Plasticity, Japan, p 145
9. Mitsuru A, Hiroto S, Yasunori H, Tatsuo S, Satoru S, Atsushi Y (1996) Patent EP 0745694 A1
10. Hall K, Kaufmann H, Mundl A (2000) In: Chiarmetta GL, Rosso M (eds) Proceedings of the 6th international conference on semi-solid processing of alloys and composites, Turin, Italy, 2000. Edimet Spa, Brescia, Italy, p 23
11. Kaufmann H, Wabusseg H, Uggowitzer PJ (2000) Aluminium 76:70
12. Xia K, Tausig G (1998) Mater Sci Eng A 246:1. doi:10.1016/S0921-5093(97)00758-2
13. Uggowitzer PJ, Kaufmann H (2004) Steel Res Int 75:525
14. Zhu MF, Kim JM, Hong CP (2001) ISIJ Int 41:992. doi:10.2355/isijinternational.41.992
15. Mitsuru A, Hiroto S, Yasunori H, Tatsuo S, Satoru S, Atsushi Y (1990) Patent EP 0,392,998A1
16. Lee SY, Lee SM, Hong CP (2000) ISIJ Int 40:48. doi:10.2355/isijinternational.40.48
17. Haga T, Kouda T, Motoyama H, Inoue N, Suzuki S (1998) In: Proceedings of the ICAA7, aluminium alloys: their physical and mechanical properties, Charlottesville, VA. Trans Tech Publications 2000 Part 1, Zurich, p 327
18. Haga T (2002) J Mater Process Technol 130–131:558. doi:10.1016/S0924-0136(02)00765-3
19. Lima Filho AD, Yamasaki MI (2006) Solid State Phenom 116–117:433
20. Ashouri S, Nili-Ahmadabadi M (2006) Solid State Phenom 116–117:201
21. Birol Y (2006) Mater Sci Forum 519–521(Part 1–2):1919
22. Birol Y (2007) J Mater Process Technol 186:94. doi:10.1016/j.jmatprotec.2006.12.021
23. Liu D, Atkinson HV, Kapranos P, Jirattiticharoean W, Jones H (2003) Mater Sci Eng A 361:213. doi:10.1016/S0921-5093(03)00528-8

24. Seidl I, Kopp R (2004) Steel Res Int 75:545
25. Pahlevani F, Nili-Ahmadabadi M (2004) Int J Cast Met Res 17:157. doi:10.1179/136404604225020560
26. Huang WD, Wang WL, Lin X, Wang M (2006) Solid State Phenom 116–117:193
27. Davis JR (ed) (1993) Speciality handbook ASM aluminium and aluminium alloys. ASM International, Materials Park, p 639
28. Haga T, Kapranos P (2002) J Mater Process Technol 118:581. doi:10.1016/S0924-0136(02)00817-8
29. Piao PY, Motegi T (2004) J Jpn Inst Met 68:228. doi: 10.2320/jinstmet.68.228
30. Haga T, Suzuki S (2001) J Mater Process Technol 118:169. doi: 10.1016/S0924-0136(01)00888-3
31. Southin RT (1967) The solidification of metals. Iron and Steel Institute, London, p 306
32. Flemings MC (1974) Solidification processing. McGraw-Hill Book Co, New York